

Numerical Investigation of the Cooling Performance of PCM-based Heat Sinks Integrated with Metal Foam Insertion

Ahmad K. AL-Migdady*, Ali M. Jawarneh, Amer Khalil Ababneh, Hussein N. Dalgamoni

Department of Mechanical Engineering, The Hashemite University, Zarqa 13133 Jordan.

Received July 24 2020

Accepted December 14 2020

Abstract

In this study, numerical simulations were carried out to analyze the cooling behavior of PCM-based heat sinks integrated with Aluminum foam. The performance of the PCM based heat sink is investigated under various operating parameters including: metal foam porosity ($\varepsilon = 100\%$, 97% and 90%), Two different PCMs (RT35HC and RT44HC) and three different values of convective heat transfer coefficient (10, 20, 30 W/m².K) while keeping the heat flux input constant at 3200 W/m². Better cooling characteristics were achieved in the heat sink filled with RT35HC when compared to RT44HC based heat sink. The Aluminum foam insertion further decreased the base temperature by almost (6 and 5)°C for the ($\varepsilon = 97\%$ and 90%) respectively when compared to the no-metal foam case ($\varepsilon = 100\%$). likewise, in the RT44HC based heat sink, a further decrease in the base temperature by almost (5 and 4)°C was reported for the ($\varepsilon = 97\%$ and 90%) cases respectively when compared to the no-metal foam case ($\varepsilon = 100\%$). The increase in the convective heat transfer coefficient resulted in longer time needed for PCM melting.

© 2021 Jordan Journal of Mechanical and Industrial Engineering. All rights reserved

Keywords: Aluminum-foam, heat sink, Phase change material "PCM", Electronic cooling;

Nomenclature

Roman Letters		Greek Letters	
A_{mush}	The mushy zone constant	α	Liquid fraction
C_p	Specific heat	β	Thermal expansion coefficient
H, h^*	Enthalpy	ε	porosity
h	Convective heat transfer coefficient	ρ	Density
k	Thermal conductivity	μ	Viscosity
K	Permeability		
L_f	Latent heat of fusion		
p	Pressure		
S_x, S_y	Darcy's Momentum sink		
t	Time		
T	Temperature		
T_s	Solidus Temperature		
T_l	Liquidus Temperature		
u	Velocity in x-direction		
v	Velocity in y-direction		

1. Introduction

The production of multi-purpose compact electronic devices was enormously increased in the past few decades. The performance of these devices is significantly reduced when their temperature is notably increased, and the challenge is to provide these components with effective thermal management systems to prevent overheat. In fact, the failure rate of electronic components is proportional to the temperature rise and according to Mithal [1], the failure decreases by 4% with a temperature rise reduction of only 1 °C. The conventional forced or natural air-cooled heat sinks that are equipped with fins are the most common ways used for electronic cooling. However, during the past few years many innovative cooling techniques had emerged including heat sinks incorporated with phase-change materials "PCM". PCMs have many advantages including: low cost, wide range of phase temperature transition and large latent heat of fusion which give these materials the ability to absorb large amount of energy with the heat sink being maintained at an almost constant temperature.

The selection for a PCM is dependent on the temperature control needs of the electronic components; since different PCMs would have various thermophysical properties including: the melting range, specific heats and latent heat of fusion.[2, 3, 4, 5, 6, 7, 8, 9]

Tan et. al [10] numerically studied the effect of power level on metallic enclosure containing PCM " n-eicosane ",

* Corresponding author e-mail: a.k.almigdady@hu.edu.jo.

the melting rate as well as the temperature rise and melting rate of the metallic casing was proportional to the power dissipation and for very low power level temperature rise was too small to cause melting, and the PCM use inside the heat sink as unjustified. Yang et al. [11] carried out a numerical study to investigate the performance of PCM-based heat sinks for various power levels, they reported that a more stable operation temperature was achieved upon the use of PCM.

Kandasamy et al. [12] numerically and experimentally investigated a heat sink filled with paraffin wax, they considered varying power dissipation levels, orientation of package to gravity, and various melting/freezing times under cyclic steady conditions. They demonstrated that melting rate is proportional to the power input, whereas the thermal performance of the heat sink was insignificantly affected by the package orientation. They also indicated that improvements of the thermal resistance of the PCM will lead to a smaller PCM package for the same cooling requirements.

The main disadvantage of PCMs is that they have low thermal conductivities, and this leads to slow heat transfer rate. To overcome this difficulty, two techniques are mainly used; the first one is concerned with increasing the heat transfer surface area, and this can be achieved mainly by equipping the heat sink with fins with various sizes, shapes and spacing, using multiple PCMs, adding metal matrix, such as metal pipes and Lessing rings to the PCM cavity and increasing the fill volume ratio. The second technique is concerned with improving the overall thermal conductivity of the integrated heat sink, and this is usually done by inserting nano-particles/nano-tubes with high thermal conductivity into the pcm[7].

Hosseinzadeh et al. [13] carried out an experimental and numerical study on the performance of heat sink equipped with internal fins, so the effects of power level, number of fins and the fin thickness were all investigated. The heat sink performance was improved with the increase of the fins number and fins height; however, such performance was little influenced by the fin thickness. Arshad et al. [14] built and tested a heat sink integrated with PCM and equipped with pin fins with square cross section. They considered three heat sinks with different fins number and thickness, but kept the volume fraction of fins to PCM at 9%. The optimum fin thicknesses were estimated for different operating conditions including input dissipating power and PCM volume fractions.

Shatikian et al. [15] performed a numerical study on a PCM based heat sink with internal fins, paraffin wax was used in this study and the results showed that the heat sink performance is highly dependent on the fin geometry as well as the fin efficiency.

Mahmoud et al. [16] experimentally studied a PCM based heat sink with different inserts. They considered six different types of PCMs and six different heat sink configurations, and they found out that heat sinks performance is enhanced with increasing number of fins, in fact, it was observed that the peak temperature was reduced with increasing the fins number. Besides, it was observed that employing honeycomb inserts with lower melting point PCM reduced the operating temperature of the heat sink and

hence, honeycomb inserts can be considered as a good alternative for replacing machined fins.

Metal foam insertions; which have low density, high porosity with high surface area to volume ratio as well as high thermal conductivity, are considered excellent thermal conductivity enhancer "TCE" for most PCM based applications such as low temperature [17, 18, 19, 20] and high temperature Latent Heat Thermal Energy Storage units "LHTES" [21, 22, 23].

In this study, the commercial Ansys-Fluent software 15.0 was used to investigate the performance of a two-dimensional configuration of a heat sink integrated with PCM and metal foam composite under three main different operating parameters: metal foam porosity, PCM type and convective heat transfer coefficient between the heat sink boundaries and the surroundings, which is to the best of the authors' knowledge, was not addressed in this approach before.

2. Physical description and mathematical formulation

The proposed configuration of the two-dimensional heat sink is illustrated in Figure 1, the heat sink is composed of a rectangular cavity ($46 \text{ mm} \times 30 \text{ mm}$) that is filled with PCM and metal foam composite and is surrounded by uniform solid enclosure of a thickness of 2 mm. A uniform, constant heat flux of 3200 W/m^2 is applied on the lower side of the metal enclosure, while all other boundaries are subjected to convection heat transfer; three values of convection heat transfer coefficient (h) were chosen in this simulation: $h = 10, 20$ and $30 \text{ W/m}^2\cdot\text{K}$. Also, two types of PCM were selected; RT35HC and RT44HC. Furthermore, to account for the metal foam variation three values of metal foam porosity were considered, $\varepsilon = 1.00, 0.97$ and 0.90 , where $\varepsilon = 1.00$ refers to no-metal foam case.

Aluminum was selected for both the metal container as well as the porous media due to low density and high thermal conductivity. The thermophysical properties of RT44HC, RT35HC, and Aluminum are listed in Table 1, while the geometric specifications of the porous media used in this study are listed in Table 2.

The size of such heat sink can be applied in practice to many electronic packages that requires cooling like microprocessors and printed circuit boards, besides, the chosen PCMs as well as metal foams are available at reasonable prices.

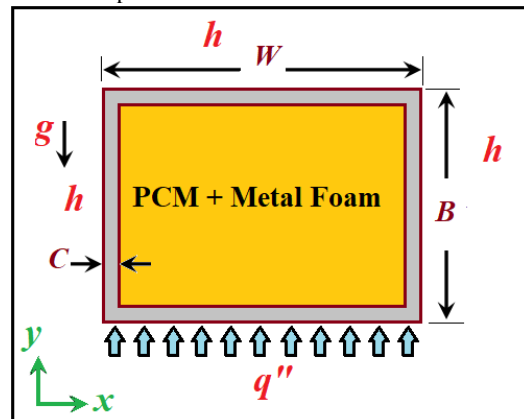


Figure 1. PCM-based heat sink configuration.

Table 1. Thermophysical properties of RT35HC, RT44HC, and Aluminum [24]

	RT35HC	RT44HC	Aluminum
Melting range (°C)	34–36	41–44	–
Latent heat (kJ/kg)	240	250	–
Density (kg/m ³)	Solid : 880 Liquid : 770	Solid : 800 Liquid : 700	2719
Specific heat (J/kg-K)	2000	2000	871
Thermal conductivity (W/m-K)	0.2	0.2	202.4
Volume expansion coefficient (1/K)	0.000865	0.00259	–
Dynamic viscosity (Pa s)	Liquid : 0.0044	Liquid : 0.008	–
Thermal diffusivity (m ² /s)	1.33 × 10 ⁻⁷	1.21 × 10 ⁻⁷	8.2 × 10 ⁻⁵

Table 2. Geometric specification of porous media [25]

Porosity	PP I	Fiber Dia (m)	Pore Dia (m)	Inertia coefficient	Permeability m ²
0.9726	5	0.00050	0.00402	0.097	2.7×10 ⁻⁷
0.9005	20	0.00035	0.00258	0.088	0.9×10 ⁻⁷

2.1. The governing equations

The physical domain was modeled based on the following assumptions:

- All materials are considered homogeneous and isotropic throughout, besides metal foams are considered rigid with open cell configuration.
- The liquid phase of PCM is considered as Newtonian and incompressible fluid with an unsteady flow; however, Boussinesq approximation was applied to account for buoyancy effects induced by density.
- PCM density is temperature independent while all other thermophysical properties are not.
- Negligible effects of viscous dissipation as well as radiation heat transfer.

Based on the above, the governing equations will be:

Mass conservation:

$$\frac{\partial u}{\partial x} + \frac{\partial v}{\partial y} = 0 \tag{1}$$

Momentum Conservation equations in horizontal and vertical directions are expressed by equation (2) and (3) respectively.

$$\begin{aligned} \frac{\rho}{\varepsilon} \frac{\partial v}{\partial t} + \frac{\rho}{\varepsilon^2} \left(u \frac{\partial u}{\partial x} + v \frac{\partial u}{\partial y} \right) &= -\frac{\partial p}{\partial x} + \frac{\mu}{\varepsilon} \left(\frac{\partial^2 u}{\partial x^2} + \frac{\partial^2 v}{\partial y^2} \right) \\ &- \left(\frac{\mu}{K} u + \frac{\rho C_f |\vec{V}|}{\sqrt{K}} u \right) - S_x \end{aligned} \tag{2}$$

$$\begin{aligned} \frac{\rho}{\varepsilon} \frac{\partial u}{\partial t} + \frac{\rho}{\varepsilon^2} \left(u \frac{\partial v}{\partial x} + v \frac{\partial v}{\partial y} \right) &= -\frac{\partial p}{\partial y} + \frac{\mu}{\varepsilon} \left(\frac{\partial^2 u}{\partial x^2} + \frac{\partial^2 v}{\partial y^2} \right) + \varepsilon \rho \beta g (T - T_{ref}) \\ &- \left(\frac{\mu}{K} v + \frac{\rho C_f |\vec{V}|}{\sqrt{K}} v \right) - S_y \end{aligned} \tag{3}$$

Where: ε , C_f and K are porosity, inertial coefficient, and permeability of the metal foam, respectively. While the terms S_x and S_y stand for source terms added to the momentum equations to account for the liquid fraction in pore volume and computed as:

$$\begin{aligned} S_x &= \frac{(1-\alpha)}{\alpha^3 + \sigma} A_{mush} u \dots (4a) \text{ and } S_y \\ &= \frac{(1-\alpha)}{\alpha^3 + \sigma} A_{mush} v \end{aligned} \tag{4b}$$

Where: A_{mush} is known as the mushy zone constant, which controls the amplitude of velocity damping and it also influences the heat transfer and flow characteristics during melting and solidification, and its value has been set at 10^5 and it usually varies within $(10^4 - 10^7)$, while σ is another constant with small value, usually 0.001, to avoid division by zero, α : the liquid fraction, and it is calculated according to

$$\alpha = \begin{cases} 0 & \text{for } T < T_s \\ \frac{T - T_s}{T_l - T_s} & T_s < T < T_l \\ 1 & \text{for } T > T_l \end{cases} \tag{5}$$

Conservation of energy for the PCM/metal foam composite can be written as

$$\left(\varepsilon \rho C_p + (1-\varepsilon) \rho_m C_{pm} \right) \frac{\partial T}{\partial t} + \varepsilon \rho L_f \frac{\partial \alpha}{\partial t} + \frac{\partial(\rho u H)}{\partial x} + \frac{\partial(\rho v H)}{\partial y} = k_{eff} \left(\frac{\partial^2 T}{\partial x^2} + \frac{\partial^2 T}{\partial y^2} \right) \tag{6}$$

Where ρ and C_p are the density, specific heat of the PCM, while ρ_m and C_{pm} are the density, specific heat of the metal foam, and k_{eff} is the effective thermal conductivity of the PCM/metal foam composite, although the literature contains numerous formulas for the effective thermal conductivity, Fluent software uses the following simple relation:

$$k_{eff} = \varepsilon k_{PCM} + (1-\varepsilon) k_m \tag{7}$$

His the enthalpy and it is the sum of sensible enthalpy “ h^* ” and the latent heat “ ΔH^* ”

$$H = h^* + \Delta H^* \tag{8}$$

The sensible enthalpy “ h^* ” and the latent heat “ ΔH^* ” are calculated using the following equations:

$$h^* = h_{ref}^* + \int_{T_{ref}}^T c_{p,eff} dT \tag{9}$$

$$\Delta H = \alpha L_f \tag{10}$$

Where $C_{p,eff}$ is the effective specific heat of the PCM/metal foam composite

$$\rho_{eff} c_{p,eff} = \varepsilon \rho_{PCM} c_{p,PCM} + (1-\varepsilon) \rho_m c_{p,m} \tag{11}$$

Where ρ_{eff} is the effective density of the PCM/metal foam composite, which is written as:

$$\begin{aligned} \rho_{eff} &= \varepsilon \rho_{PCM} + (1-\varepsilon) \rho_m \end{aligned} \tag{12}$$

The specific heat of PCM is given by the following equation

$$C_p = \begin{cases} C_{ps} & \text{for } T \leq T_s \\ C_{ps}(1 - \alpha) + C_{ps}(\alpha) + \frac{\Delta H}{T_l - T_s} & T_s < T < T_l \\ C_{pl} & \text{for } T \geq T_l \end{cases} \quad (13)$$

Here, C_{ps} , C_{pl} , T_s , T_l , and ΔH are the specific heat of solid, specific heat of liquid, solidus temperature, liquidus temperature, and latent heat of the PCM, respectively.

2.2. Numerical setup: initial and boundary conditions

At the start of the simulation the whole arrangement is in thermal equilibrium with surroundings at $T_\infty = 298 \text{ K}$, also horizontal and vertical components of velocity are zero; $u = v = 0$.

As simulation proceeds, the following boundary conditions are considered:

- At the container walls, horizontal and vertical components of velocity are zero; $u = v = 0$
- Continuous heat flux at the outer “cold” enclosure boundaries; *cold boundaries: upper, left and right sides of the enclosure and the hot boundary: the heated lower side.*

$$-k \frac{\partial T}{\partial n} = h(T - T_\infty) \quad (14)$$

- Continuous heat flux between the inner container boundaries and PCM-foam composite interfaces, as:

$$-\left(k \frac{\partial T}{\partial n}\right)_{PCM} = -\left(k \frac{\partial T}{\partial n}\right)_{Al} \quad (13)$$

The physical problem described above was modeled, and governing equations were solved using Ansys Fluent 15.0 commercial software which uses the enthalpy-porosity technique to model the phase change process. In this technique, the liquid fraction, which is associated with each control volume in the domain, is computed at each iteration by applying enthalpy balance. The liquid-solid mushy zone is treated as a porous zone with porosity equal to the liquid fraction, and appropriate momentum sink terms are added to the momentum equations to account for the pressure drop caused by the presence of solid material.

Initially, both the system and the surroundings are in thermal equilibrium at 298 K; this thermal equilibrium is disturbed by imposing a constant heat flux of 3200 W/m^2 at the lower side of the metal enclosure and the convective heat transfer boundary condition was applied on all the other enclosure sides. A quadrilateral mesh of about 13600 elements was suitable of all cases with time step of 0.2 seconds.

2.3. Model Validation

The numerical approach was validated by simulating an independent model and comparing to the work of Sunuku et al.[24]. Their work included the simulation of a two-dimension heat sink ($30 \text{ cm} \times 50 \text{ cm}$) with an Aluminum enclosure of 2.0 mm thickness, the heat sink was further subdivided by 2 vertical slabs of 2.0 mm thickness each and space created by the enclosure was filled with RT44HC with the base being subjected to a constant heat flux. The time evolution of melt fraction for three values of constant heat flux for the current work and that of Sunuku[24] are presented in Figure 2 and a satisfactory agreement between the results of the two works exists.

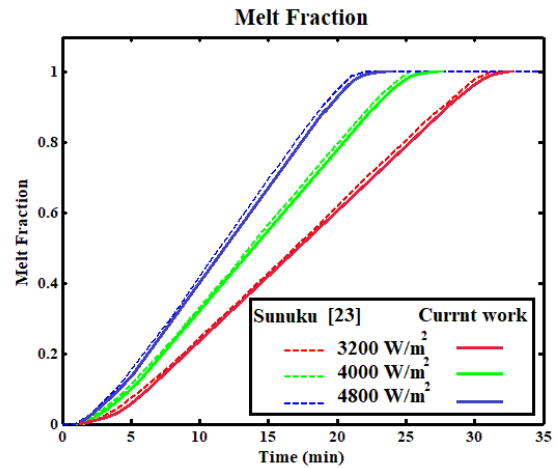


Figure 2. Average melt fraction variation with time, comparison between this study and that of Sunuku[24].

3. Data and results

As mentioned earlier, the PCM based heat sink was studied for a fixed heat flux of 3.2 kW/m^2 , two PCM types: RT35HC and RT44HC and three porosity values: $\epsilon = 1.00$, 0.97 and 0.90, where $\epsilon = 1.00$ refers to no-metal foam case. Besides, convection heat transfer takes place at outer enclosure cold sides with the surroundings, three values of the convective heat transfer coefficient were considered: $h = 10, 20$ and $30 \text{ W/m}^2\text{K}$. Figures 3 and 4 show the time evolution of melt fraction and the average base temperature variation with time for the RT35HC and RT44HC heat sinks integrated with metal foam ($\epsilon = 1.00, 0.97$ and 0.90) and convective heat transfer coefficient of $10 \text{ W/m}^2\text{K}$. In the no-metal foam case ($\epsilon = 1.00$), PCM starts receiving heat from the adjacent hot surface and its temperature rises in that vicinity and once the melting temperature is reached, it starts melting. At the early stages of melting conduction heat is much significant and as melting continues, the solid region size gets smaller and conduction is present in the solid matrix while convection dominates the heat transfer process within the molten region. In fact, convection currents are formed due to buoyancy effects caused by temperature gradients and consequently mixing is enhanced and the PCM is eventually totally melted. During the melting process, the PCM temperature rise is limited by its solidus and liquids temperature range and accordingly the base temperature variation is low, and the base temperature profile has a small slope during melting.

Melting starts sooner in the no-metal foam case ($\epsilon = 1.00$) since metal foam insertion enhances heat transfer from the base and the PCM cavity to the cold sides of the container, in other words, the thermal conductivity is enhanced with the addition of the porous media. Indeed, melting time is inversely proportional to porosity, besides, the base temperature rise during melting is inversely proportional to porosity as well. The time required for melting was (47, 37, 34) minutes for ($\epsilon = 1.00, 0.97$ and 0.90) cases respectively. However, base temperature variation within the melting region was approximately between (42°C and 43°C), (37°C and 38°C) and (36°C and 37°C) for ($\epsilon = 1.00, 0.97$ and 0.90) cases respectively. In other words, a base temperature reduction of about (5–6) $^\circ\text{C}$ was achieved by using high porosity metal foams. However,

the base temperature difference during melting between the ($\epsilon = 0.97$ and 0.90) cases was only 1°C .

A similar behavior was noted in the RT44HC cases, where base temperature variation within the melting region was approximately between (48°C and 50°C), (44°C and 45°C) and (43°C and 44°C) for ($\epsilon = 1.00, 0.97$ and 0.90) cases respectively and a base temperature reduction of about ($4\text{--}5$) $^\circ\text{C}$ was achieved by using high porosity metal foams and again the base temperature difference during melting between the ($\epsilon = 0.97$ and 0.90) cases was about only 1°C . However, the estimated time for melting was ($44, 39, 37$) minutes for ($\epsilon = 1.00, 0.97$ and 0.90) cases respectively.

Figure 5 illustrates the effect of heat transfer coefficient on the cooling performance of heat sink filled with RT35HC. As the convective heat transfer increases, the rate of heat rejection from the heat sink increases and the PCM needs more time to melt. For the convective heat transfer coefficient value of $20\text{ W/m}^2\cdot\text{K}$ the melting time was ($50, 40, 37$) minutes for the ($\epsilon = 1.00, 0.97$ and 0.90) cases respectively, whereas for the $30\text{ W/m}^2\cdot\text{K}$ value the melting time was ($43, 40$) minutes for ($\epsilon = 0.97$ and 0.90) cases respectively, however, the simulation was terminated for the ($\epsilon = 1.00$) case at 50 minutes and melt fraction was about 92% .

Figure 6 shows the time evolution of temperature distribution within the RT35HC based heat sink for cases of $\epsilon = 1.00$ and $\epsilon = 0.97$ at convective heat transfer coefficient of $20\text{ W/m}^2\cdot\text{K}$. In the no-metal foam case, heat is transferred from heat source and container boundaries to the cavity, and PCM starts melting in the outer region towards the center. In fact, the container boundaries contribute to a significant amount of heat to be transferred to the PCM due to the high thermal conductivity of the Aluminum enclosure compared to that of the PCM. At the same time, the rest of heat is dissipated at the container outer cold sides by convection. With continuous heating, the PCM at the cavity boundaries is totally molten and its temperatures rises, nevertheless, less heat is received by the center of the PCM due to its low thermal conductivity hence slight increase in temperature is observed with slow propagation rate of the molten region.

Upon the addition of metal foam, thermal conductivity of the PCM is remarkably enhanced as well as heat transfer rate through the PCM towards the container boundaries, as a result the temperature distribution within PCM and enclosure boundaries becomes more uniform. Besides, as it can be noted from figure 6, the container base temperature as well as that of the container boundaries are reduced when compared to the no-metal foam case. In fact, upon the addition of metal foam, thermal conductivity within the PCM cavity is enhanced and consequently heat flow towards the container cold sides is significantly improved and hence better cooling is achieved upon enhanced heat rejection at the outer sides of the enclosure.

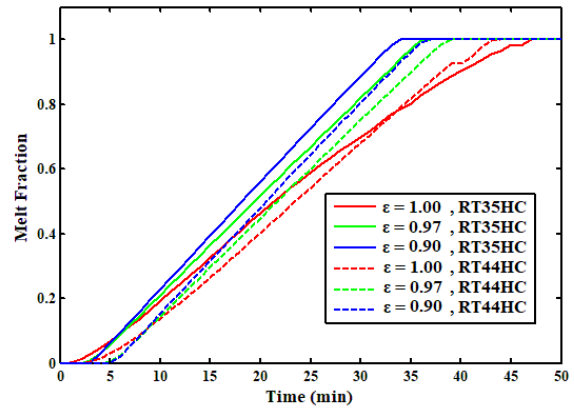


Figure 3. Time variation of Average melt fraction at $h=10\text{W/m}^2\cdot\text{K}$.

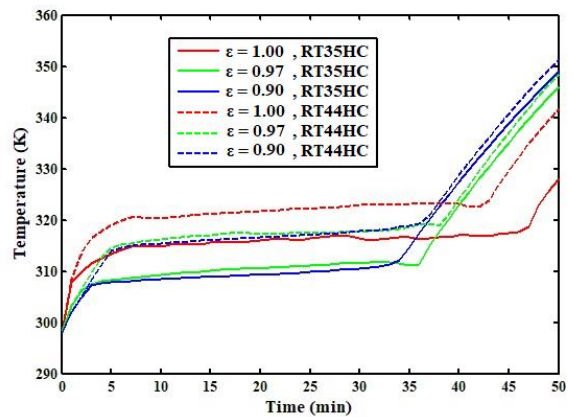


Figure 4. Time variation of the average base temperature at $h=10\text{W/m}^2\cdot\text{K}$.

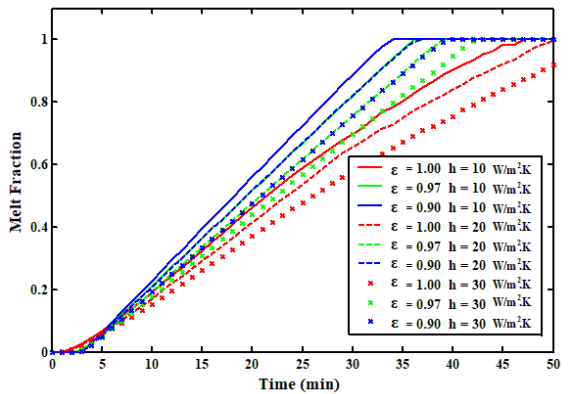


Figure 5. Time variation of the average melt fraction for the RT35HC based heat sink for different values of convective heat transfer coefficients.

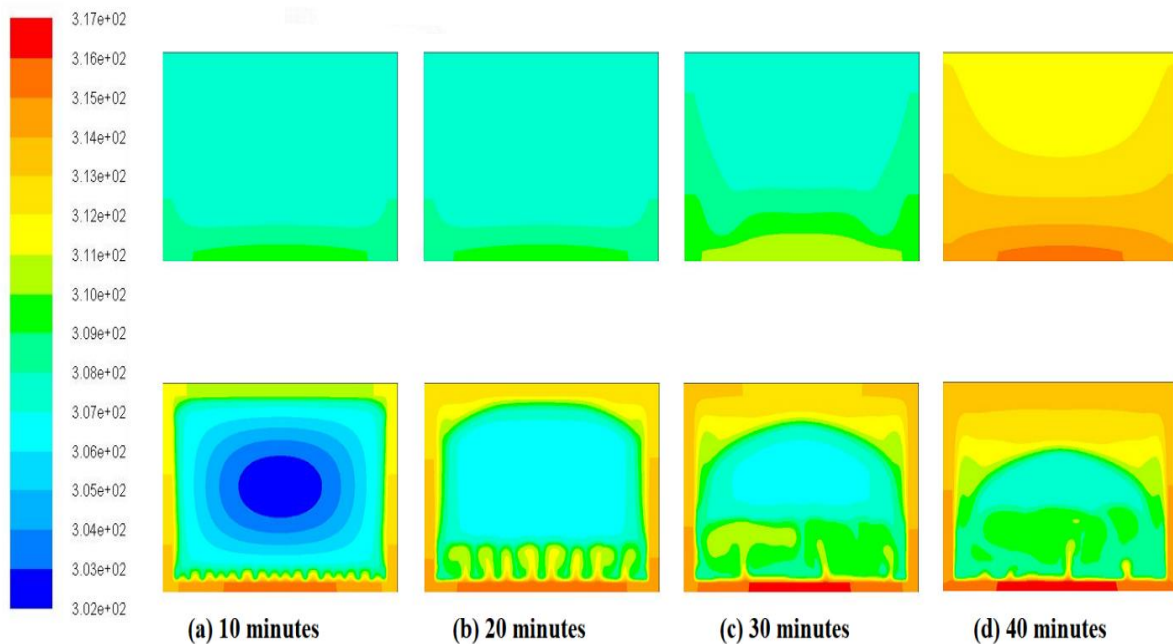


Figure 06. Evolution of temperature contours for the RT35HC based heat sink at a convective heat transfer coefficient of $20 \text{ W/m}^2\text{K}$; $\epsilon = 0.97$ top row, $\epsilon = 1.00$ bottom row.

Conclusions

The metal foam insertion significantly enhanced the performance of the heat sink, it improved the overall thermal conductivity within the enclosure cavity, increased the heat transfer rate from the hot surface towards the cold sides of the metal enclosure and caused a more uniform temperature distribution within the PCM. In fact, the improved heat transfer out of the heat sink resulted in temperature reduction in both the hot and cold sides of the enclosure, besides, the melting time was also reduced as well.

In the RT35HC based heat sink, the Aluminum foam insertion of (0.97 and 0.90) porosity caused a base temperature reduction of (5 and 6) $^{\circ}\text{C}$ respectively when compared to that of no-metal foam case with the three values of convective heat transfer coefficient.

In the RT44HC based heat sink, the Aluminum foam insertion of (0.97 and 0.90) porosity caused a base temperature reduction of (4 and 5) $^{\circ}\text{C}$ respectively when compared to that of no-metal foam case with the three values of convective heat transfer coefficient.

Increasing the convective heat transfer coefficient reduced the melting rate of the PCM due to the heat rejection increase from cold sides of the heat sink and kept the base at reduced temperature for longer duration.

References

- [1] P. Mithal, "Design of experimental based evaluation of thermal performance of a flichip electronic assembly," *ASME EEP Proceedings. New York: ASME*, vol. 18, p. 109–15, 1996.
- [2] S. Sahoo, M. Das and P. Rath, "Application of TCE-PCM based heat sinks for cooling of electronic components: A review," *Renewable and Sustainable Energy Reviews*, vol. 59, pp. 550–582, 2016.
- [3] M. Kensarian, "High-temperature phase change materials for thermal energy storage," *Renewable Sustainable Energy Reviews*, vol. 14, p. 955–970, 2010.
- [4] H. Ge, H. Li, S. Mei and J. Liu, "Low melting point liquid metals as a new class of phase change material: an emerging energy frontier," *Renewable Sustainable Energy Reviews*, vol. 21, p. 331–346, 2013.
- [5] S. Khare, M. Dell'Amico, C. Knight and S. McGarry, "Selection of materials for high temperature latent heat energy storage," *Solar Energy Materials & Solar Cells*, vol. 107, p. 20–27, 2012.
- [6] M. A. Y. C. Wang X. Q., "Effect of orientation for phase change material (PCM)-based heat sinks for transient thermal management of electric components," *International Communications in Heat and Mass Transfer*, vol. 34, no. 7, p. 801–808, 2007.
- [7] A. K. AL-Migdady, A. M. Jawarneh, H. N. Dalgamoni and M. Tarwaneh, "Combined Effects of Eccentricity and Internal Fins on the Shell and Tube Latent Heat Storage Systems," *International Journal of Recent Technology and Engineering (IJRTE), Volume-9 Issue-1, May 2020*, vol. 9, no. 1, pp. 230–236, 2020.
- [8] M. Hamdan, M. Shehadeh, A. Al Aboushi, A. Hamdan and E. Abdelhafez, "Photovoltaic Cooling Using Phase Change Material," *Jordan Journal of Mechanical and Industrial Engineering*, vol. 12, no. 3, pp. 167–170, 2018.
- [9] M. M. Al-Maghalseh, "Investigate the Natural Convection Heat Transfer in A PCM," *Jordan Journal of Mechanical and Industrial Engineering*, vol. 11, no. 4, pp. 217–223, 2017.
- [10] F. Tan and C. Tso, "Cooling of mobile electronic devices using phase change materials," *Applied Thermal Engineering*, vol. 24, p. 159–169, 2004.
- [11] Y. Yang and Y. Wang, "Numerical simulation of three-dimensional transient cooling application on a portable

- electronic device using phase change material," *International Journal of Thermal Sciences*, vol. 51, p. 155–162, 2012.
- [12] R. Kandasamy, X. Wang and A. Mujumdar, "Application of phase change materials in thermal management of electronics," *Applied Thermal Engineering*, vol. 27, p. 2822–2832, 2007.
- [13] S. Hosseinizadeh, F. Tan and S. Moosania, "Experimental and numerical studies on performance of PCM-based heat sink with different configurations of internal fins," *Applied Thermal Engineering*, vol. 31, no. 17-18, p. 3827–3838, 2011.
- [14] A. Arshad, H. Ali, W. Yan, A. Hussein and M. Ahmadlouydarab, "An experimental study of enhanced heat sinks for thermal management using n-eicosane as phase change material," *Applied Thermal Engineering*, vol. 132, no. 5, pp. 52-66, 2018.
- [15] V. Shatikian, M. Ziskind and R. Letan, "Numerical investigation of a PCM-based heat sink with internal fins," *International Journal of Heat and Mass Transfer*, vol. 48, p. 3689–3706, 2005.
- [16] S. Mahmoud, A. Tang, C. Toh, R. AL-Dadah and S. Soo, "Experimental investigation of inserts configurations and PCM type on the thermal performance of PCM based heat sinks," *Applied Energy*, vol. 112, p. 1349–1356, 2013.
- [17] W. Li, Z. Qu, Y. He and W. Tao, "Experimental and numerical studies on melting phase change heat transfer in open-cell metallic foams filled with paraffin," *Applied Thermal Engineering*, vol. 37, p. 1–9, 2012.
- [18] S. Mancin, A. Diani, L. Doretto, K. Hooman and L. Rossetto, "Experimental analysis of phase change phenomenon of paraffin waxes embedded in copper foams," *International Journal of Thermal Sciences*, vol. 90, pp. 79-89, 2015.
- [19] B. Zalba, J. Marín, L. Cabeza and H. Mehling, "Review on thermal energy storage with phase change materials, heat transfer analysis and applications," *Applied Thermal Engineering*, vol. 23, no. 3, p. 251–283, 2003.
- [20] C. Zhao, W. Lu and Y. Tian, "Heat transfer enhancement for thermal energy storage using metal foams embedded within phase change materials (PCMs)," *Solar Energy*, vol. 84, no. 8, p. 1402–1412, 2010.
- [21] J. Yang, X. Du, L. Yang and Y. Yang, "Numerical analysis on the thermal behavior of high temperature latent heat thermal energy storage system," *Solar Energy*, vol. 98, p. 543–552, 2013.
- [22] J. Yang, L. Yang, C. Xu and X. Du, "Numerical analysis on thermal behavior of solid-liquid phase change within copper foam with varying porosity," *International Journal of Heat and Mass Transfer*, vol. 84, p. 1008–1018, 2015.
- [23] C. Zhao and Z. Wu, "Heat transfer enhancement of high temperature thermal energy storage using metal foams and expanded graphite," *Solar Energy Materials & Solar Cells*, vol. 95, p. 636–643, 2011.
- [24] J. Sunku Prasad, R. Anandalakshmi and P. Muthukumar, "Numerical investigation on conventional and PCM heat sinks under constant and variable heat flux conditions," *Clean Techn Environ Policy*, 2020.
- [25] V. V. Calmidi and M. R. L., "Forced convection in high porosity metal foams," *Journal of Heat Transfer*, vol. 122, no. 3, pp. 557-565, 2000.